Molecular Cancer Therapeutics

A Urokinase Receptor–Derived Peptide Inhibiting VEGF-Dependent Directional Migration and Vascular Sprouting

Katia Bifulco[1], Immacolata Longanesi-Cattani[1], Eleonora Liguori[1], Claudio Arra[1], Domenica Rea[1], Maria Teresa Masucci[1], Mario De Rosa[2], Vincenzo Pavone[3], Maria Patrizia Stoppelli[4], and Maria Vincenza Carriero[1]

Abstract

The receptor for the urokinase-type plasminogen activator (uPAR) is a widely recognized master regulator of cell migration, and $uPAR_{88–92}$ is the minimal sequence required to induce cell motility. We previously showed that soluble forms of uPAR elicit angiogenic responses through their $uPAR_{88–92}$ chemotactic sequence and that the synthetic peptide SRSRY exerts similar effects. By a drug design approach, based on the conformational analysis of the $uPAR_{88–92}$ sequence, we developed peptides (pERERY, RERY, and RERF) that potently inhibit signaling triggered by $uPAR_{88–92}$. In this study, we present evidence that these peptides are endowed also with a clear-cut antiangiogenic activity, although to different extents. The most active, RERF, prevents tube formation by human endothelial cells exposed to SRSRY. RERF also inhibits VEGF-triggered endothelial cell migration and cord-like formation in a dose-dependent manner, starting in the femtomolar range. RERF prevents F-actin polymerization, recruitment of αvβ3 integrin at focal adhesions, and αvβ3/VEGFR2 complex formation in endothelial cells exposed to VEGF. At molecular level, the inhibitory effect of RERF on VEGF signaling is shown by the decreased amount of phospho-FAK and phospho-Akt in VEGF-treated cells. *In vivo*, RERF prevents VEGF-dependent capillary sprouts originating from the host vessels that invaded angioreactors implanted in mice and neovascularization induced by subcorneal implantation of pellets containing VEGF in rabbits. Consistently, RERF reduced the growth and vascularization rate of tumors formed by HT1080 cells injected subcutaneously in the flanks of nude mice, indicating that RERF is a promising therapeutic agent for the control of diseases fuelled by excessive angiogenesis such as cancer. *Mol Cancer Ther; 12(10); 1981–93. ©2013 AACR.*

Introduction

Angiogenesis is a complex multistep process leading to the formation of new blood vessels from a pre-existing vascular network. In adults, angiogenesis is a well-regulated process. Conversely, an abnormal neoangiogenesis occurs during the pathogenesis of several chronic diseases like diabetes, rheumatoid arthritis, and cancer (1). Tumor angiogenesis is critical to the growth of solid tumors, as they would remain in a dormant phase for a long time in the absence of new vessel formation (2). Therefore, interfering with angiogenic signals is a logical approach for the treatment of solid cancers. Inhibition of angiogenesis was first proposed as a therapeutic strategy against malignancies by Folkman in 1971 (3). Thereafter several antiangiogenic strategies have been developed, and the combination of various angiogenesis inhibitors with other targeted therapies has been explored in preclinical and clinical trials (4).

Because of to its prominent role in triggering angiogenesis, the VEGF soluble factor has been the focus of many studies. Currently, 4 molecular-targeted drugs interfering on VEGF pathways are approved by the U.S. Food and Drug Administration for 6 different tumor indications (5). VEGF acts primarily through VEGFR2, regulates endothelial cell migration, proliferation, differentiation, and survival, as well as vessel permeability, by activating multiple signaling mediators including focal adhesion kinase (FAK), mitogen-activated protein kinase (MAPK), Akt, PLC-γ, and Src family kinases (6). VEGF-induced and VEGFR2-mediated FAK phosphorylation regulates assembly and disassembly of focal adhesions, actin organization, and leads, together with paxillin and actin-anchoring proteins such as vinculin, to recruitment of this kinase to focal adhesions (7).

Integrins of the β_3 subfamily specifically bind to the extracellular domain of VEGFR-2 resulting in increased

Authors' Affiliations: [1]Department of Experimental Oncology, National Cancer Institute of Naples; [2]Department of Experimental Medicine, Second University of Naples; [3]Department of Chemical Sciences, University "Federico II" of Naples; and [4]Institute of Genetics and Biophysics "Adriano Buzzati-Traverso", National Research Council, Naples, Italy

Note: Supplementary data for this article are available at Molecular Cancer Therapeutics Online (http://mct.aacrjournals.org/).

Corresponding Author: Maria Vincenza Carriero, Department of Experimental Oncology-National Cancer Institute of Naples, via M. Semmola, Naples 80131, Italy. Phone: 390-8159-03569; Fax: 390-8159-03814; E-mail: m.carriero@istitutotumori.na.it.

doi: 10.1158/1535-7163.MCT-13-0077

receptor activation upon VEGF stimulation (8). The αvβ3 vitronectin receptor is minimally expressed on resting or normal blood vessels but is significantly upregulated on vascular cells within human tumors or in response to growth factors (9).

By virtue of its ability to regulate integrin distribution at the leading edge, urokinase-type plasminogen activator receptor (uPAR) has been shown to be a key component of the network through which VEGF controls endothelial cell migration (10). As a glycosylphosphatidylinositol-anchored protein (11), the uPAR lacks transmembrane and intracellular domains and, therefore, uPAR must cooperate with transmembrane receptors such as formyl peptide receptors (FPR) and integrins to signal (12, 13).

Many human cancers overexpress uPAR, and elevated levels of intact or cleaved soluble forms of uPAR (SuPAR) in body fluids or tumor lysates frequently correlate with poor prognosis in cancer (14–17). The role of uPAR in angiogenesis is well documented, by virtue of its ability to focus urokinase proteolytic activity on cell surface and modulate cell migration (18, 19). We have recently shown that SuPAR stimulates, in a protease-independent manner, *in vitro* and *in vivo* angiogenesis, through its $uPAR_{88–92}$ chemotactic sequence (20).

The Ser^{88}-Arg-Ser-Arg-Tyr^{92} ($uPAR_{88–92}$) sequence, located on the external surface of uPAR, is a protease-sensitive region which retains a strong chemotactic activity even in the form of an isolated peptide (SRSRY; refs. 21, 22). Mechanistically, $uPAR_{88–92}$ sequence promotes cell motility by interacting with G-protein–coupled FPRs which, in turn, trigger vitronectin receptor activation with an inside-out type of mechanism (21, 22).

Previous work from this laboratory highlighted specific amino acid substitutions of Ser^{90} in the full-length uPAR that interfere with the complex cross-talk involving uPAR, FPR, and vitronectin receptor (23). Also, penta- and tetrapeptides carrying Ser^{90} substituted with a glutamic acid residue inhibit signaling triggered by the $uPAR_{88–92}$ sequence (24, 25). Among these, the N-terminal acetylated and C-terminal amidated Ac-Arg-Glu-Arg-Phe-NH_2 peptide, namely RERF, potently inhibits *in vitro* and *in vivo* cell migration and invasion of human fibrosarcoma HT1080 cells without affecting cell proliferation. Cell exposure to RERF results in the inhibition of both uPAR/FPR and uPAR/vitronectin receptor interactions (25). These effects are supported by the identification of FPR as the main binding site of RERF and αv integrin subunit as a low affinity-binding site (K_{dsapps}, 10^{-17} and 10^{-13} mol/L, respectively).

In this study, we show that p-ERERY, RERY, and the most active RERF synthetic peptides behave as antiangiogenic agents which inhibit responses promoted by the $uPAR_{88–92}$ sequence, as well as by VEGF, starting in the femtomolar range. In endothelial cells exposed to VEGF, RERF prevents F-actin polymerization, recruitment of αvβ3 integrin at the focal adhesions, and phosphorylation of several proteins such as FAK and Akt. We also present evidence that RERF prevents VEGF-dependent endothelial tube formation and vascular sprouting in angioreactors implanted in nude mice and neovascularization in rabbits corneas. Antiangiogenic effect of RERF was confirmed by the analysis of growth and vascularization of tumors formed by HT1080 cells injected subcutaneously in the flanks of nude mice.

Materials and Methods

Peptide synthesis and purification

Peptides, synthesized by the solid phase approach using standard Fmoc methodology in a manual reaction vessel, were purified by RP-HPLC-C18 column to a 99% purity, and molecular weights were confirmed by mass spectrometry as previously described (25).

Cell cultures

Human umbilical vein endothelial cells (HUVEC) were purchased by Lonza, which provided a certificate of analysis for each cell lot. This guarantees the expression of CD31/105, von Willebrand Factor VIII, and VEGFR2 through 15 population doublings. HUVECs, used between the third and the seventh passage according to Arnaoutova and colleagues (26), were grown in Eagle Basal Medium (EBM) supplemented with 4% FBS, 0.1% gentamicin, 1 μg/mL hydrocortisone, 10 μg/mL EGF, and 12 μg/mL bovine brain extract (Cambrex). Human fibrosarcoma HT1080 cells were grown in Dulbeccos' Modified Eagle's Media (DMEM) + 10% FBS and were passaged for less than 6 months. Although HT1080 cells were not subjected to genetic authentication, their characteristic morphology, uPAR expression, and VEGF secretion were specifically verified. Also, their ability to migrate toward VEGF and the amino-terminal fragment of uPA as well as their matrix-invading ability *in vitro* was checked not more than 3 months before their use (23).

Soluble human uPAR was purified from the conditioned medium of mouse LB6/hSuPAR cells (27) and quantified by ELISA as described (28). LB6/hSuPAR cells were a gift of F. Blasi (IFOM, Milan, Italy). Within 1 month of receipt, LB6/hSuPAR cells were grown in DMEM–10% FBS for several passages and aliquots of each were frozen. For preparation of conditioned medium, LB6/hSuPAR cells were thawed and grown for no more than 5 passages. Both HT1080 and LB6/hSuPAR cells were tested for mycoplasma contamination (Mycoplasma Plus PCR Primer Set, Stratagene; Agilent Technologies Inc).

Motility assay

Cell migration assays were conducted using Boyden chambers and 8-μm pore size polyvinylpyrrolidone-free polycarbonate filters (Nucleopore) as previously described (20). Briefly, HUVECs were detached, counted, and seeded in the upper chamber at 7×10^4 cells per well (95%–98% viable cells) in EBM. The lower chamber was filled with EBM, with or without 40 ng/mL $VEGF_{165}$, (Becton Dickinson), 10 nmol/L SuPAR, or synthetic peptides at the indicated concentrations. Other experiments were carried out using cells preincubated for 30 minutes at

37°C with 1 μg/mL anti-human VEGF polyclonal antibody (Ab) neutralizing the biologic activity of $VEGF_{165}$ and $VEGF_{121}$ (R&D Systems) or cells desensitized with 100 nmol/L fMLP for 30 minutes at 37°C in humidified air with 5% CO_2 (20). Incubation was carried out for 4 hours at 37°C in humidified air with 5% CO_2. At the end of the assay, the migrated cells on the lower filter surfaces were fixed with ethanol, stained with hematoxylin, and counted in 10 random fields/filter at ×200 magnification.

Endothelial cell tube formation assay

The formation of vascular-like structures was assessed on Matrigel as described (20). HUVECs were suspended in 300 μL prewarmed EBM. Diluents or effectors were added to the cell suspension before seeding cells (4×10^4 cells/well) on plates coated with 300 μL/well growth factor–reduced Matrigel (Becton Dickinson). SuPAR or $VEGF_{165}$ were used at 10 nmol/L or 40 ng/mL concentrations, respectively. Assays were conducted for 6 hours at 37°C in humidified air with 5% CO_2. When indicated, cells were preincubated for 30 minutes at 37°C with 5 μg/mL LM609 anti-αvβ3 mAb or 1 μg/mL anti-human VEGF Ab. Other experiments were carried out in the presence of 1 nmol/L recombinant endostatin (Sigma-Aldrich), a 20-kDa C-terminal fragment of type XVIII collagen with potent *in vitro* and *in vivo* antiangiogenic activity (29). Complete capillary tube network within a designated area of a low magnification field was observed under light microscopy. To quantify tube formation, 5 random areas per well at 100× magnification were imaged, and the number of tubes formed by cord-like structures exceeding 100 μm in length (30) was counted using Axiovision 4.8 software (Carl Zeiss). Unless otherwise specified, the net contribution of each effector or antibody in promoting tube formation was calculated as a percentage of tube-like structures counted in the absence of any angiogenic stimulus (EBM), considered as 100%.

Fluorescence microscopy

HUVECs grown on glass coverslips to semiconfluence were starved for 60 minutes in EBM. Then, cells were exposed to EBM alone, 40 ng/mL $VEGF_{165}$ or 40 ng/mL $VEGF_{165}$ mixed to 10 nmol/L ERFR or 10 nmol/L RERF for 30 minutes at 37°C in humidified air with 5% CO_2. Slides were washed with PBS, fixed, and permeabilized with 2.5% formaldehyde–0.1% Triton X-100 in PBS for 10 minutes at 4°C. After several washes in PBS, slides were incubated with 2 μg/mL anti-vinculin mAb (clone VIIF9 purchased from Chemicon) and then with 1:800 goat Alexa Fluor 488 anti-mouse IgG (Molecular Probes) at 23°C for 60 and 45 minutes, respectively. Thereafter, 2 μg/mL LM609 anti-αvβ3 mAbs (Chemicon) and 1:800 diluted rabbit Alexa Fluor 594 anti-mouse IgG (Molecular Probes) were applied to slides at 23°C for 60 and 45 minutes, respectively. To analyze cytoskeletal organization, coverslips were incubated with 0.1 μg/mL rhodamine-conjugated phalloidin (Invitrogen) at 23°C for 45 minutes. In all cases, slides were mounted using 20% (w/v) mowiol and cells visualized with a 510 META-LSM confocal microscopy (Carl Zeiss). To visualize phosphorylation of FAK, cells were exposed to EBM alone, 40 ng/mL $VEGF_{165}$, or 40 ng/ml $VEGF_{165}$ mixed to 10 nmol/L ERFR or 10 nmol/L RERF for 15 minutes at 37°C in humidified air with 5% CO_2. Then, cells were fixed, permeabilized, and incubated with anti-phospho-FAK (Tyr397) Ab (p-FAK) purchased from Millipore, and goat Alexa Fluor 488 anti-rabbit IgG (Molecular Probes) at 23°C for 60 and 45 minutes, respectively. After nuclear staining with 4′, 6-diamidino-2-phenylindole (DAPI), cells were analyzed by a fluorescence-inverted microscope connected to a videocamera (Carl Zeiss).

Western blotting and phospho-kinase array

HUVECs grown to semiconfluence were starved for 18 hours in 0.2% FBS EBM. Then, cells were exposed to EBM alone, 40 ng/mL $VEGF_{165}$ with/without 10 nmol/L ERFR or 10 nmol/L RERF at 37°C in humidified air with 5% CO_2. At the indicated times, cells were lysed in radioimmunoprecipitation assay (RIPA) buffer (10 mmol/L Tris pH 7.5, 140 mmol/L NaCl, 0.1% SDS, 1% Triton X-100, 0.5% NP40) containing 5 mmol/L Na_3VO_4 and a protease inhibitor mixture (Sigma-Aldrich). Cell lysate protein content was measured by a colorimetric assay (BioRad). Western blot analysis was conducted as previously described (23). Briefly, 50 μg proteins were separated on 7.5% SDS-PAGE and transferred onto a polyvinylidene fluoride membrane. The membranes were blocked with 5% non-fat dry milk and probed with anti p-FAK Ab or anti-phospho-Akt (Ser473) (p-AKT) Ab (Cell Signaling) and then with anti-FAK mAb (Millipore) or anti-Akt mAb (R&D Systems). In all cases, washed filters were incubated with horseradish peroxidase–conjugated anti-mouse or anti-rabbit antibody and detected by enhanced chemiluminescence kit (Amersham). Densitometry was conducted by NIH Image 1.62 software (Bethesda, MD). The effects of VEGF with ERFR or RERF combinations were analyzed at the level of global kinase phosphorylation, using the dot-blot Proteome Profiler Array Human PhosphoKinase Array Kit (R&D Systems), according to manufacturer's instructions. Briefly, 200 μg of protein was applied on each membrane, and the signals were detected as described for Western blotting. The pixel density of each spot was measured using NIH Image 1.62 software. The intensity of positive control spots was used to normalize results between the three membranes. The intensity for each spot was then averaged over the duplicate spots.

Cell adhesion assay

Cell adhesion assays were conducted using 24-well tissue culture plates coated with 5 μg/mL vitronectin, diluted in PBS, and incubated overnight at 4°C. The plates were rinsed with PBS, incubated for 1 hour at 23°C with 1% bovine serum albumin (BSA) in PBS, and rinsed again. HUVEC (1×10^5 cells/well) were plated in each coated well and incubated for 2 hours at 37°C, 5% CO_2 in serum-free EBM, 40 ng/mL $VEGF_{165}$ with/without

10 nmol/L ERFR or 10 nmol/L RERF. After 3 washes with PBS, adherent cells were detached and counted.

Co-immunoprecipitation of αv/uPAR complexes

Cells exposed for 30 minutes to 40 ng/mL $VEGF_{165}$ with/without 10 nmol/L RERF or diluents at 37°C were lysed in RIPA buffer (23). Extracts (400 μg/sample) were incubated overnight at 4°C with 5 μg/mL anti-VEGFR2 Ab (Cell Signaling). Proteins co-purified with VEGFR2 were recovered by Protein G-Sepharose and analyzed by a 6% SDS-PAGE followed by Western blotting with 1 μg/mL VNR139 anti-αv mAb (Chemicon) or 2 μg/mL anti-VEGFR2 Ab.

Survival assay

HUVECs (2×10^3/well) were seeded in 96-well tissue culture plates and left to adhere in complete media for 3 hours, then rinsed twice with PBS, and incubated with complete growth medium or EBM mixed to 40 ng/mL $VEGF_{165}$ with or without the indicated peptides. Medium with or without peptides was replaced every 24 hours. After 72 hours, suspended cells were removed and the adherent cells were stained with MTT dye (Sigma-Aldrich) for 4 hours at 37°C, as described (25). The absorbance was determined at 570 nm using a microplate reader (Biorad). With a similar experimental design, endothelial cell proliferation was assessed using 16-well plates and the xCELLigence Technology (Roche Diagnostics) as described (31). The impedance value of each well was automatically monitored by the xCELLigence system and expressed as a cell index value.

In vivo angiogenesis assays

The DIVAA (Trevigen) Assay Kit was used as a quantitative *in vivo* method to assay angiogenesis as described (32). Silicone cylinders of 20 μL volume (angioreactors) were filled with an extract containing extracellular matrix mixed with PBS, 10 nmol/L SRSRY, 12.5 ng VEGF with or without 10 nmol/L the indicated peptides, or 10 μg/mL endostatin. Twelve CD1 female nude mice (Harlan; 23 to 25 g) 6 to 8 weeks old were maintained in a germ-free environment. Housing and handling of mice were in accordance with institutional guidelines complying with national and international laws and policies. Two angioreactors were implanted subcutaneously in the dorsal region of each CD1 nude mouse. Fifteen days after the implantation, mice were sacrificed and angioreactors were removed. The vessel-containing matrix was removed from the cylinders. Cells recovered by digestion with dispase were stained using FITC-lectin, and endothelial cells were quantified by fluorescence at 510 nm emission with 485 nm excitation using Victor 3 fluorimeter (Perkin Elmer), according to the manufacturer's instructions.

For the corneal pocket assay, twelve female New Zealand White rabbits (Charles River) weighing 2.5 to 3.0 kg were used. Rabbits were anesthetized by intramuscular injection of acepromazina (1 mg/kg), ketamine hydrochloride (35 mg/kg), and xilazina hydrochloride (5 mg/kg), and 3 to 4 drops of 0,4% ossibuprocain chlorohydrate solution were topically applied to the eye before micropocket surgery. A wire speculum was positioned in the eye, and a sucralfate hydron pellet containing PBS or 180 ng VEGF with/without 5 μg RERF was implanted into the cornea after making a micropocket in the stroma, using standard surgical tools (33). TobraDex (0.3% tobramycin-0.1% dexamethasone) was applied to the surface of the cornea after pellet implantation to prevent infection. Observation and quantification of the angiogenic response were conducted by a slit-lamp stereomicroscope. The angiogenic activity was evaluated on the basis of the number and growth rate of newly formed capillaries. An angiogenic score of 1 corresponded to 0–25 vessels per cornea, 2 from 25–50, 3 from 50–75, 4 from 75–100, and 5 for >100 vessels.

Growth and vascularization of tumor in mice

To evaluate the effect of RERF on tumor growth and vascularization, highly invasive fibrosarcoma HT1080 cells were injected as a single-cell suspension (1×10^6 cells in 70 μL of sterile PBS, 97% viability), subcutaneously in the flanks of ten $Foxn1^{nu/nu}$ mice (Harlan). Animals were randomized into 2 groups of 5 with the treatment group receiving 3 mg/kg RERF by i.v. injection every 48 hours and the control group receiving an equivalent injected volume of vehicle (PBS) only. Mice weight was monitored and time-dependent average weight was monitored every 5 days. The length and the width of the tumors were measured at different time points with the help of a caliper, and the volume was calculated using the formula: $^1/_2 \times (\text{width})^2 \times \text{length}$ (mm). After 20 days, animals were sacrificed and excised tumors were fixed in buffered formalin and processed for paraffin sectioning. Tumor vascularization was assessed by counting vascular channels harboring red blood cells on hematoxylin and eosin–stained sections in 5 randomly chosen fields per section, in at least 2 sections per tumor at ×200 magnification.

Statistical analysis

The results are expressed as the means ± SD of the number of the indicated determinations. Data were analyzed by *t* test for multiple comparisons. $P < 0.001$ was accepted as significant.

Results

RERF inhibits endothelial cell migration and tube formation stimulated by the uPAR chemotactic sequence

Previous work from this laboratory has shown that SuPAR stimulates *in vitro* and *in vivo* angiogenesis through its Ser^{88}-Arg-Ser-Arg-Tyr^{92} chemotactic sequence ($uPAR_{88–92}$), in a protease-independent manner (20) and that penta- and tetrapeptides (pERERY, RERY and RERF) carrying the Ser^{90} substituted with a glutamic acid residue

inhibit $uPAR_{88–92}$–dependent signaling (24, 25). As endothelial cell migration is a recognized step of angiogenesis, we first investigated the possibility that these uPAR-derived peptide inhibitors may counteract SuPAR-triggered angiogenic response.

By conventional Boyden chamber assays, we evaluated the effects of pERERY, RERY, and RERF peptides on cell migration of HUVECs exposed to the $uPAR_{88–92}$ motogen stimulus. According to previously reported data (20), we found that 10 nmol/L SuPAR or 10 nmol/L SRSRY elicited a considerable endothelial cell migration, reaching 190% and 180% of the basal cell migration. The addition of equimolar concentrations of pERERY, RERY, or RERF reduced cell migration by 38%, 52%, and 52%, respectively. Similarly, 53% inhibition of SRSRY-dependent cell migration was achieved by 10 nmol/L RERF. In all cases, control penta- or tetrapeptides (ARARY and ERFR peptides) were ineffective (Fig. 1A). Endothelial cells undergo morphologic differentiation into an extensive network of capillary-like structures consisting of highly organized 3-dimensional cords when seeded on Matrigel in the presence of a pro-angiogenic stimulus. To analyze the effect of these peptide inhibitors on tube formation, HUVECs were plated on Matrigel in the presence of 10 nmol/L SuPAR or 10 nmol/L SRSRY, and the appearance of tubular branches was assessed after 6 hours. For each experiment, the newly formed cord-like structures assessed in the presence of Matrigel alone was considered as 100% (35 ± 10/well tube-like structures exceeding 100 μm in length). In accordance with previous data, we found that both SuPAR and SRSRY elicited a similar response, reaching 191% and 184%, respectively, above basal (Fig. 1B and C). The addition of RERY or RERF peptides, used at 10 nmol/L, reduced SuPAR-dependent endothelial cell capillary-like structures by 43% and 49%, respectively, whereas ERFR control peptide was ineffective. Similarly, RERY and RERF reduced SRSRY-triggered endothelial cell tube formation by 41% and 47%, respectively (Fig. 1B and C). These findings prompted us to test and characterize the antiangiogenic properties of RERF.

RERF inhibits VEGF-dependent migration and cytoskeletal reorganization of endothelial cells

Because the uPAR is an essential component of the network through which VEGF controls endothelial cell migration (10), we investigated the effect of RERF on VEGF-triggered signaling. First, the ability of RERF to prevent VEGF-directed HUVEC migration was tested by a

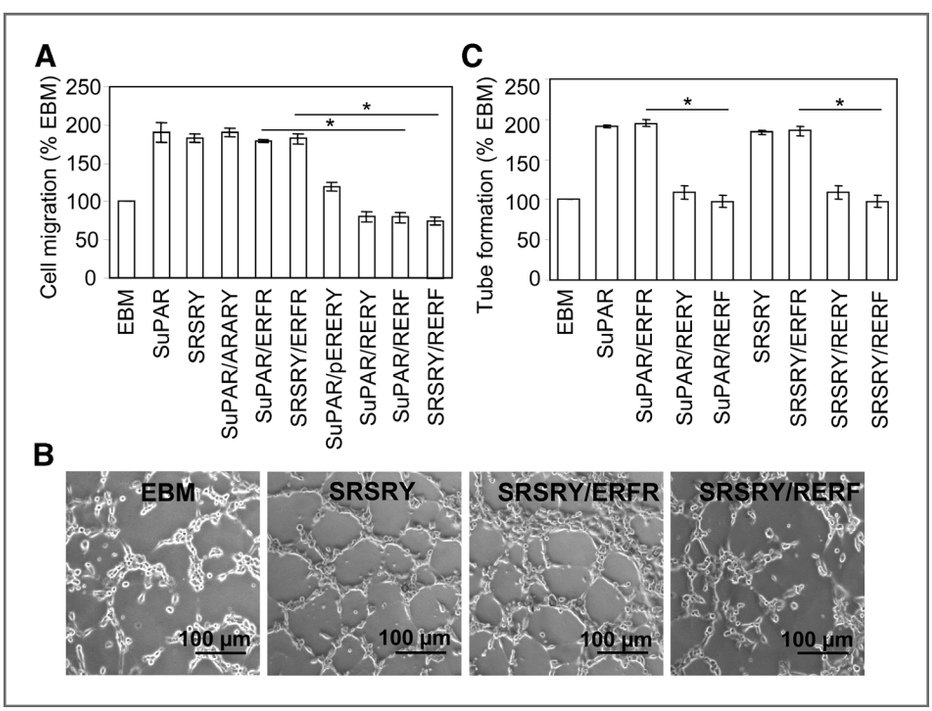

Figure 1. RERF inhibits endothelial cell migration and tube formation stimulated by the $uPAR_{88–92}$ chemotactic sequence. A, HUVECs were allowed to migrate in Boyden chambers toward 10 nmol/L SuPAR or 10 nmol/L SRSRY peptide with or without equimolar concentration of the indicated peptides for 4 hours at 37°C in 5% CO_2. The extent of cell migration was expressed as a percentage of the cell migration in the absence of chemoattractants (EBM, considered as 100%). Data are expressed as the mean ± SD of 3 independent experiments, carried out in duplicate. *, $P < 0.0001$. B, HUVECs were suspended in prewarmed EBM, with or without 10 nmol/L SuPAR or 10 nmol/L SRSRY in the presence or the absence of equimolar concentrations of the indicated peptides, then seeded on Matrigel-coated plates at 37°C. Tube formation was observed after 6 hours. Representative pictures were taken with an inverted microscope. Original magnifications, ×100. C, quantitative analysis of tube formation was expressed as a percentage of tubes formed by cord-like structures exceeding 100 μm in length, counted in the absence of any angiogenic stimulus, considered as 100% (EBM). The data are expressed as the means ± SD of 3 independent experiments carried out in duplicate. *, $P < 0.001$.

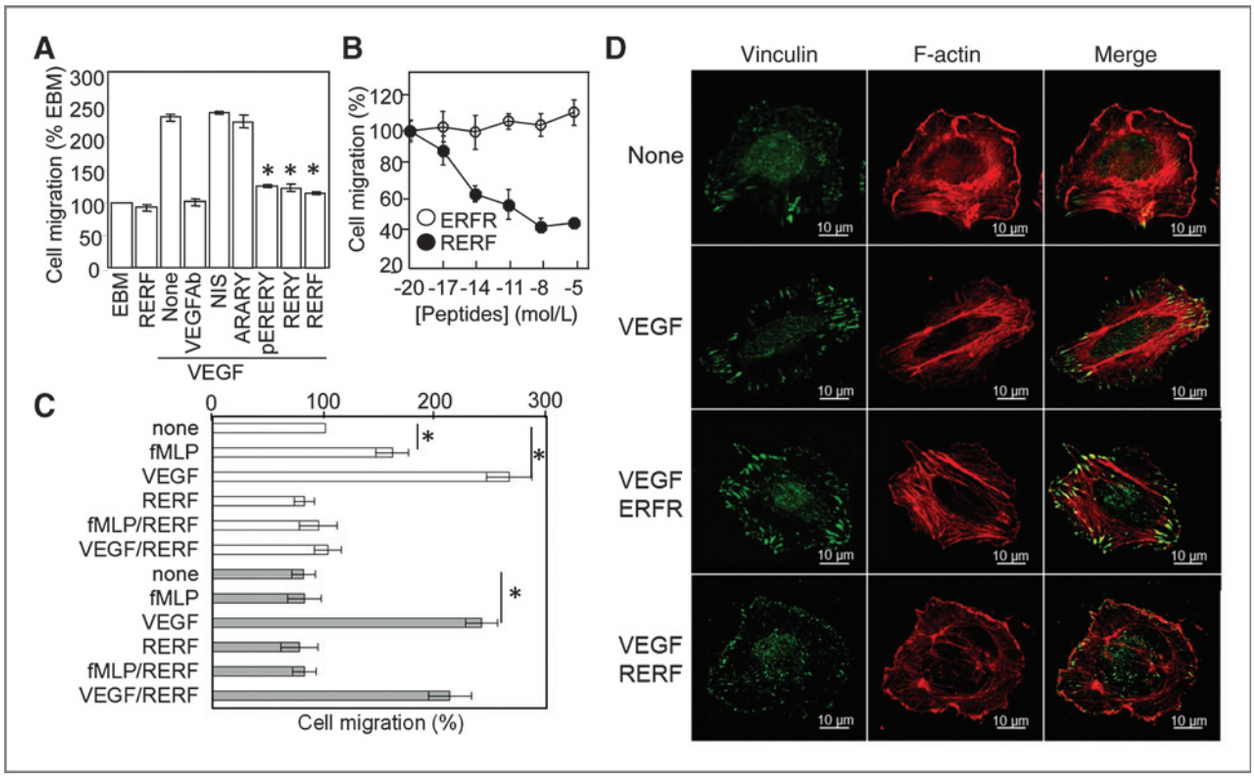

Figure 2. RERF inhibits migration and cytoskeletal organization of endothelial cells stimulated by VEGF. HUVECs were allowed to migrate in Boyden chambers for 4 hours at 37°C in 5% CO_2 toward diluents (EBM), 10 nmol/L RERF, or 40 ng/mL $VEGF_{165}$ with or without 5 μg/mL nonimmune serum (NIS), 1 μg/mL anti-human VEGF Ab, 10 nmol/L or increasing concentrations of indicated peptides. A, the extent of cell migration was expressed as a percentage of the cell migration assessed in the absence of any chemoattractant (EBM), considered as 100%. *, $P < 0.001$ in respect to cell migration toward $VEGF_{165}$ alone (None). B, the extent of cell migration was expressed as a percentage of the net $VEGF_{165}$-dependent cell migration, considered as 100%. In all cases, data are expressed as the means ± SD of 3 independent experiments, carried out in duplicate. C, HUVECs were incubated with diluents (white column) or with 100 nmol/L fMLP (grey column) for 30 minutes at 37°C in humidified air with 5% CO_2 and then allowed to migrate toward 10 nmol/L RERF, 10 nmol/L fMLP, or 40 ng/mL $VEGF_{165}$ with or without 10 nmol/L RERF. The extent of cell migration was expressed as a percentage of the cell migration assessed in the absence of any chemoattractant (none = 100%). *, $P < 0.001$ in respect to cell migration toward EBM (None). D, representative confocal images of HUVECs grown on glass slides to semiconfluence, exposed to diluents (None), 40 ng/mL $VEGF_{165}$, or 40 ng/mL $VEGF_{165}$ mixed to 10 nmol/L ERFR or 10 nmol/L RERF for 30 minutes at 37°C and double stained for vinculin and F-actin. Original magnification, ×630.

Boyden chamber assay. We found that 40 ng/mL $VEGF_{165}$ elicited endothelial cell migration up to 240% of the basal cell migration, whereas RERF alone reduced migration slightly below the basal level. The combination of $VEGF_{165}$ with 10 nmol/L pERERY, RERY, or RERF reduced cell migration by 46%, 50%, and 52%, respectively, whereas the control peptides ARARY or ERFR were ineffective. Interestingly, the extent of RERF inhibition was similar to that exerted by anti-VEGF Ab (Fig. 2A). Unlike ERFR control peptide, RERF inhibits VEGF-directed migration of endothelial cells in a dose-dependent manner. The inhibition starts in the low femtomolar concentration range and plateaus in the nanomolar range (Fig. 2B). FPR is the main binding site of RERF (25). To investigate whether FPR has a role in the inhibitory effect on VEGF-dependent endothelial cell migration, we blocked FPR function by desensitizing HUVECs with an excess of fMLP and then analyzed their ability to migrate toward VEGF in the presence or in the absence of RERF. We found that desensitized HUVECs retain the ability to respond to the motogen effect of VEGF, showing that FPR is not needed for VEGF-dependent migration. In contrast, only a slight inhibitory effect was exerted by RERF, indicating that FPR activity is indispensable for the inhibitory capability of RERF (Fig. 2C).

VEGF-dependent mitogenic activity is the result of marked cytoskeletal reorganization and accumulation of stress fibers associated with new actin polymerization and rapid formation of focal adhesions (34). Accordingly, HUVECs exposed to 40 ng/mL $VEGF_{165}$ acquired a more elongated and polarized morphology as compared with unstimulated cells (Fig. 2D). The exposure of endothelial cells to VEGF induced a marked reorganization of actin into stress fibers spanning the length of the cells, most of which co-localized with vinculin-positive focal adhesions. VEGF-dependent cytoskeletal organization was still observed in HUVECs exposed to 40 ng/mL $VEGF_{165}$ mixed with 10 nmol/L ERFR, whereas VEGF-induced effects on cytoskeleton were prevented by 10 nmol/L RERF. In the latter case, endothelial cells had a condensed,

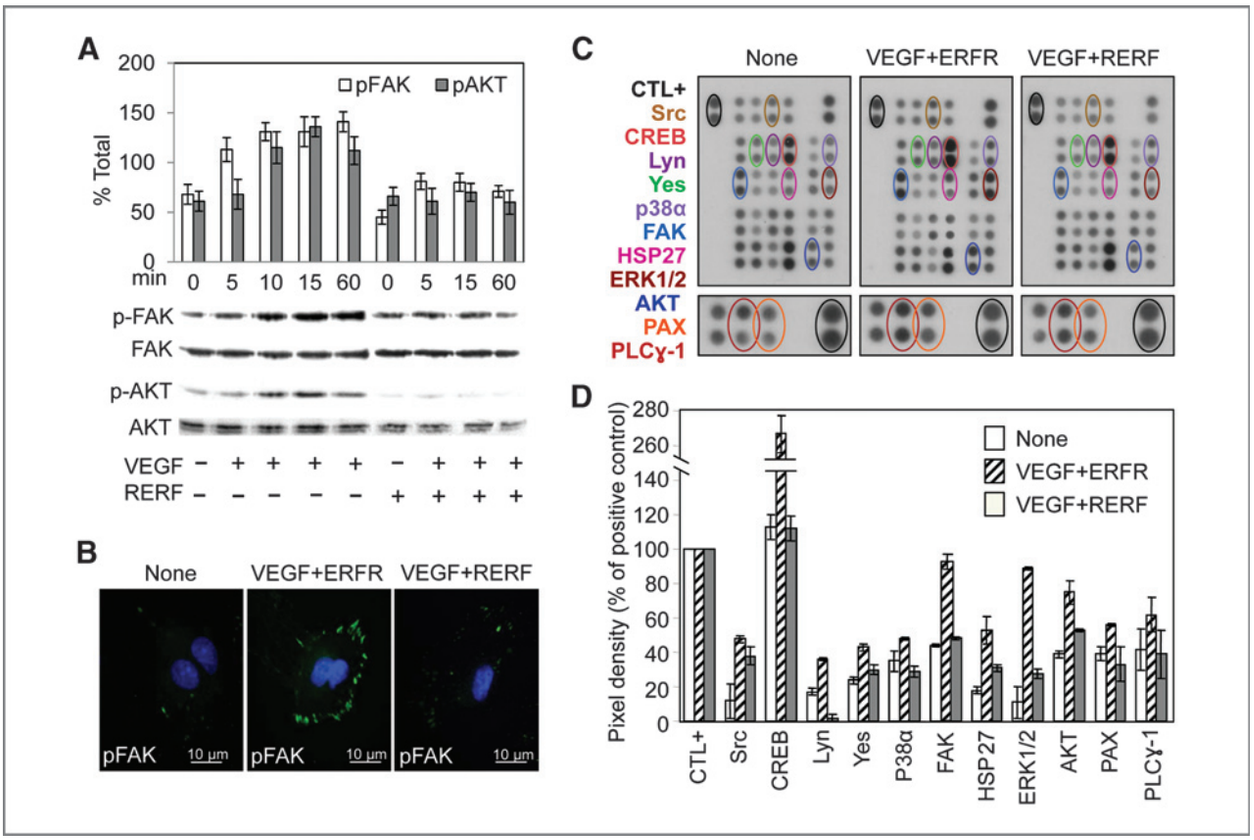

Figure 3. RERF inhibits intracellular protein phosphorylation of endothelial cells stimulated by VEGF. HUVECs grown on glass slides to semiconfluence were exposed to EBM, 40 ng/mL $VEGF_{165}$ with/without 10 nmol/L ERFR or 10 nmol/L RERF at 37°C in humidified air with 5% CO_2 for the indicated times (A) or 15 minutes (B and C). A, whole-cell lysates (50 μg/sample) immunoblotted with anti-phospho-FAK (pFAK) or anti-phospho-Akt (pAKT) Abs and then with total anti-FAK (FAK) or total anti-Akt (AKT) mAbs. The enclosed bar graph shows the average quantification of the pFAK and pAKT content expressed as a percentage of total FAK and total AKT, respectively, from 3 independent experiments. B, representative images of HUVECs double stained for pFAK and DAPI. Original magnification, ×1,000. C, analysis of HUVEC cell lysates (200 μg/sample) by a phospho-kinase array. Stained circles indicate the relevant results. D, quantification of phospho-kinase array. The pixel density of each spot was measured using NIH Image 1.62 software. The intensity of positive control spots (CTL+) was used to normalize results between the 3 membranes. Data expressed as percentage of each positive control were averaged over the duplicate spots.

rounded morphology; similarly to untreated cells, the F-actin was condensed into fewer fibers and was completely absent from the leading edges of the cells (Fig. 2D). These findings raise the hypothesis that RERF may inhibit VEGF-dependent signaling.

RERF inhibits VEGF-dependent intracellular protein phosphorylation of endothelial cells

VEGF has been shown to induce the phosphorylation of many proteins (35). To investigate the effects of RERF on the phosphorylation of VEGF intracellular targets like FAK and Akt, HUVECs were exposed to EBM or 40 ng/mL $VEGF_{165}$ with or without 10 nmol/L RERF for 0 to 60 minutes, and phosphorylated proteins were detected by Western blotting. We found that 10 nmol/L RERF consistently decreased the $VEGF_{165}$-induced and time-dependent increase of FAK and Akt phosphorylation (Fig. 3A). Accordingly, p-FAK staining dramatically decreased in focal adhesions of endothelial cells exposed for 15 minutes to $VEGF_{165}$ mixed to RERF, as compared with endothelial cells exposed to $VEGF_{165}$ mixed to ERFR (Fig. 3B). To further characterize the inhibition of VEGF-triggered signaling by RERF, VEGF-dependent phosphorylation of protein kinases in the presence of 10 nmol/L ERFR or 10 nmol/L RERF for 15 minutes was investigated with a dot blot human phospho-kinase array kit. As expected, an appreciable increase in the phosphorylation of many proteins was observed in the presence of $VEGF_{165}$ combined with ERFR peptide. In accordance with data showed in Fig. 3A, we observed an RERF-dependent marked reduction in FAK and Akt phosphorylation (51% and 30% inhibition, respectively; Fig. 3C and D). Moreover, we detected changes in the phosphorylation of some other proteins in cells exposed to $VEGF_{165}$ mixed to RERF. As shown in Fig. 3C and D, RERF caused a consistent reduction of phosphorylated Src(Y419), CREB (S133), Lyn(Y397),Yes(Y426), p38α(T180/Y182), HSP27 (S78/S82), as well as ERK1/2, all recognized mediators

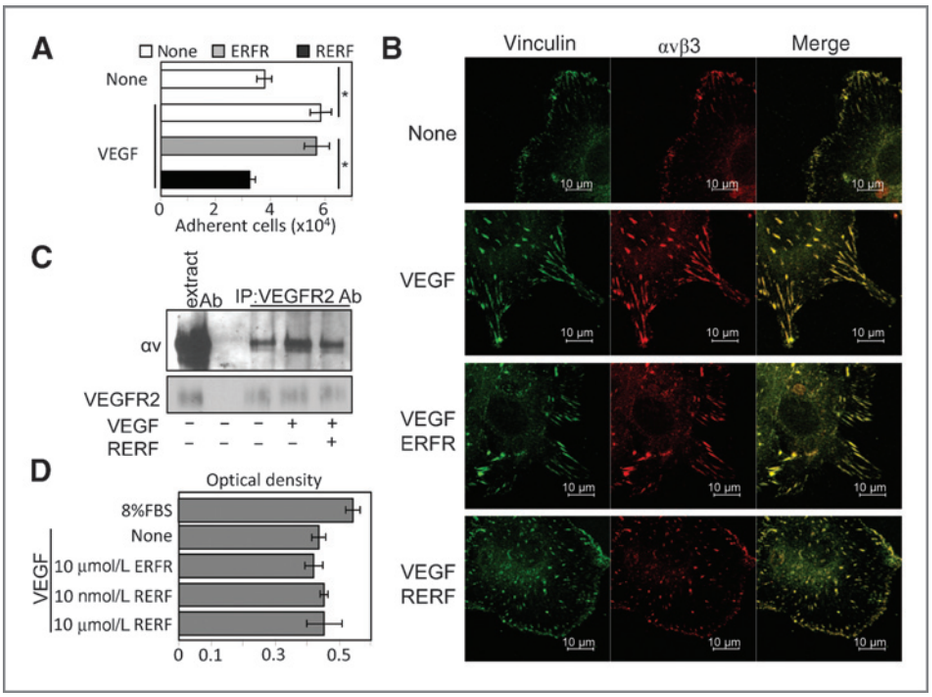

Figure 4. RERF prevents VEGF-induced endothelial cell adhesion on vitronectin and causes disappearance of αvβ3 localization at focal adhesions without affecting cell survival. A, HUVECs (1×10^5/well) were allowed to adhere for 2 hours at 37°C, 5% CO_2 on 24-well dishes coated with vitronectin in serum-free EBM (none) or 40 ng/mL $VEGF_{165}$ with/without 10 nmol/L ERFR or 10 nmol/L RERF. Data are reported as number of adherent cells and represent the average of 3 different experiments carried out in duplicate. *, $P < 0.0001$. B, representative confocal images of HUVECs grown on glass slides to semiconfluence, exposed to diluents (None), 40 ng/mL $VEGF_{165}$, or 40 ng/mL $VEGF_{165}$ mixed to 10 nmol/L ERFR or 10 nmol/L RERF for 30 minutes at 37°C and double stained for vinculin and αvβ3 integrin. Original magnification, ×630. C, lysates (400 μg/sample) from HUVECs exposed for 30 minutes to diluents or 40 ng/mL $VEGF_{165}$ with/without 10 nmol/L RERF at 37°C were immunoprecipitated with 5 μg/mL anti-VEGFR2 Ab. The resulting proteins were analyzed by Western blot using VNR139 anti-αv mAb or anti-VEGFR2 Ab. Seventy micrograms of cell extract and 0.1 μg anti-VEGFR2 Ab were loaded as control. D, proliferation of HUVECs left to adhere in complete media for 3 hours and then allowed to grow in complete media or EBM mixed to 40 ng/mL $VEGF_{165}$ with or without the indicated peptides for 72 hours. Medium with or without peptides was replaced every 24 hours. Absorbance of adherent cells was assessed by MTT assay. Data represent the mean ± SD of 2 experiments, carried out in quadruplicate.

of the VEGF-triggered signal transduction pathway. Noteworthy, VEGF-dependent phosphorylation of other protein kinases such as STAT1, STAT2, and STAT5 was not changed by cell exposure to RERF.

RERF inhibits VEGF-dependent adhesion to vitronectin and causes disappearance of αvβ3 from focal adhesions without affecting cell survival

It is known that in response to VEGF, β3 integrin regulates FAK phosphorylation, integrin-dependent actin reorganization, and leads αvβ3–VEGFR2 complexes to localize at new formed focal adhesions (36). Because it is widely accepted that αvβ3 integrin has a prominent role in the activity of VEGF and, in general, in angiogenesis, we attempted to investigate whether this integrin is indeed involved in the inhibitory activity of RERF. First, we analyzed the effect of RERF on VEGF-dependent endothelial cell adhesion to vitronectin and αvβ3 localization at focal contacts. As shown in Fig. 4A, HUVECs moderately adhere to vitronectin and cell adhesion is increased in the presence of 40 ng/mL $VEGF_{165}$. In contrast, 10 nmol/L RERF prevents endothelial cell adhesion onto vitronectin, whereas ERFR is ineffective (Fig. 4A). To explore the effect of RERF on αvβ3 localization, adherent endothelial cells were exposed to 40 ng/mL $VEGF_{165}$ in the presence or in the absence of 10 nmol/L RERF or 10 nmol/L ERFR and, after 30 minutes, vinculin and integrin αvβ3 were visualized by immunofluorescence. In agreement with the role of αvβ3 as a mediator of VEGF signaling, upon endothelial cell exposure to VEGF, αvβ3 localized at vinculin-positive focal adhesions. The addition of 10 nmol/L ERFR did not modify integrin redistribution, whereas RERF caused the loss of αvβ3 from vinculin-positive focal adhesions. Furthermore, RERF promoted the appearance of thin, αvβ3-positive linings at the cell edge, similarly to untreated cells (Fig. 4B). We have shown that RERF binds to the αv integrin subunit (25). Therefore, we investigated whether RERF inhibits VEGF-induced αvβ3-VEGFR2 complex formation by a co-immunoprecipitation experiment. As shown in Fig. 4C, an appreciable amount of VEGFR2 co-purified with αv was observed in endothelial cells, which increased upon cell exposure to 40 ng/mL $VEGF_{165}$ for 30 minutes. In contrast, in endothelial cells exposed to a combination of 40 ng/mL $VEGF_{165}$ and 10 nmol/L RERF, the extent of αv co-purified with VEGFR2 did not increase (Fig. 4C). In conclusion, these results show that

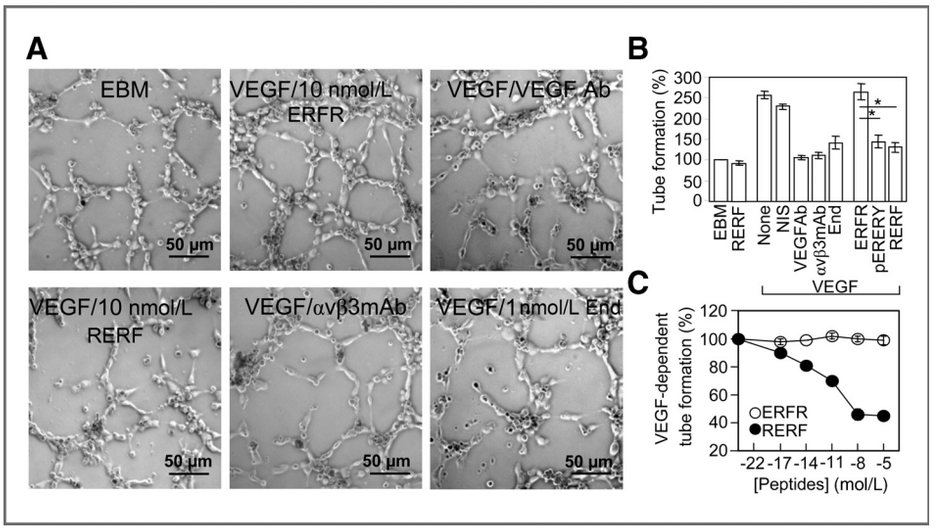

Figure 5. Dose-dependent inhibitory effect of RERF on VEGF-dependent endothelial tube formation. HUVECs were suspended in prewarmed EBM, with or without 10 nmol/L RERF, or 40 ng/mL $VEGF_{165}$ in the presence or the absence of 5 μg/mL nonimmune serum (NIS), 1 μg/mL anti-human VEGF Ab, 5 μg/mL anti-αvβ3 mAb, clone LM609, 1 nmol/L endostatin (End), or the indicated peptides at 10 nmol/L concentration and seeded on Matrigel-coated plates for 6 hours at 37°C. A, representative pictures were taken with an inverted microscope at ×200 magnifications. B, quantitative analysis of tube formation was indicated as a percentage of tubes formed by cord-like structures exceeding 100 μm in length, counted in the absence of any angiogenic stimulus considered as 100% (EBM). The data are expressed as the means ± SD of 3 independent experiments carried out in duplicate. *, $P < 0.0001$ C, tube formation of HUVECs suspended in EBM with 40 ng/mL $VEGF_{165}$ and increasing concentrations of ERFR or RERF before seeding on Matrigel-coated plates for 6 hours. Quantitative analysis was conducted as in B. Numbers are the percentages of tubular branches counted in the presence of $VEGF_{165}$ alone, considered as 100%. The data are expressed as the means ± SD of 2 independent experiments carried out in duplicate.

RERF prevents VEGF-dependent cell adhesion to vitronectin, αvβ3 re-localization, and VEGFR2/αv association, suggesting that αvβ3 may be a mediator of RERF antiangiogenic effects.

Integrin αvβ3 is an important survival system for nascent blood vessels during angiogenesis and VEGF mitogenicity has been reported to be enhanced by αvβ3-mediated endothelial cell adhesion (37, 38). A possible hypothesis is that RERF could reduce endothelial cell proliferation rate enhanced by 40 ng/mL $VEGF_{165}$. In agreement with our previous data (25), 10 μmol/L RERF did not modify the growth of endothelial cells exposed to VEGF up to 72 hours assessed by MTT assays (Fig. 4D), as well as by proliferation curves automatically monitored with the xCELLigence system (Supplementary Fig. S1).

RERF inhibits VEGF-dependent endothelial cell tube formation

To investigate whether RERF could inhibit VEGF-triggered angiogenesis *in vitro*, endothelial cells were plated on Matrigel in the presence of diluents (EBM), 10 nmol/L RERF, or 40 ng/mL $VEGF_{165}$ mixed to diluents or different combinations of effectors. After 6 hours, basal tube formation by endothelial cells exposed to EBM or 10 nmol/L RERF was comparable and taken as 100%. In contrast, endothelial cells exposed to VEGF formed a 3-dimensional network of tubes resembling capillary-like structures reaching 257% ± 10% of branches counted in the absence of any angiogenic stimulus (Fig. 5A and B). Unlike ERFR control peptide, endothelial cell incubation with anti-VEGF Ab, anti-αvβ3 mAb, or endostatin reduced VEGF-dependent tube formation to the basal level (Fig. 5A and B). The addition of 10 nmol/L pERERY or 10 nmol/L RERF reduced VEGF-dependent tube formation by 44% and 50%, respectively. Similarly to the cell migration data, RERF reduced the extent of VEGF-dependent tube formation in a dose-dependent manner. The inhibitory effect starts in the low femtomolar range and levels off in the nanomolar range, 50% of maximal effect being reached at 10 pmol/L (Fig. 5C). All together, these findings suggest that RERF could prevent VEGF-driven angiogenesis *in vivo*.

RERF inhibits angiogenesis *in vivo*

We used the DIVAA assay, which allows a quantitative assessment of angiogenesis *in vivo* as previously described (20). Matrigel-containing angioreactors were loaded with diluents, 10 nmol/L SRSRY, 12.5 ng VEGF, with or without 10 nmol/L RERF or 10 μg/mL endostatin and implanted into the dorsal flank of nude mice. Angioreactors were recovered after 15 days, and capillary sprouts originating from the host vessels that invaded angioreactor were quantified by measuring fluorescence-associated to endothelial cells, following staining with fluorescein isothiocyanate (FITC)-lectin. As expected, both SRSRY and VEGF generated a remarkable angiogenic response, although to a different extent, as compared with controls (Fig. 6A). RERF reduced capillary sprouts originating by SRSRY or VEGF to a similar extent (Fig. 6A). Measurement

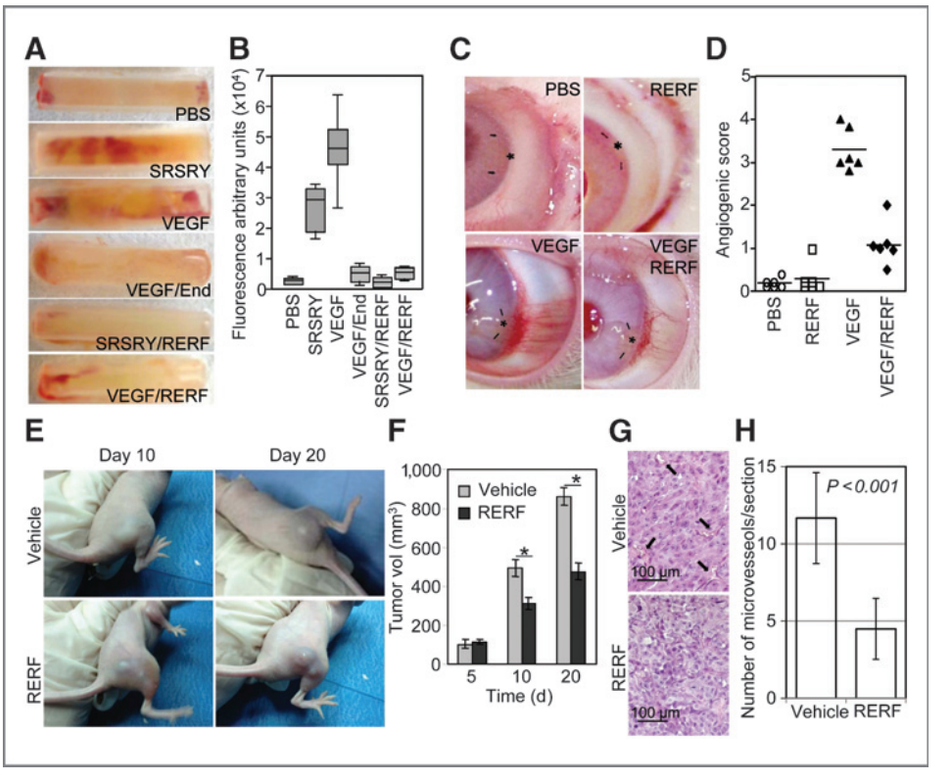

Figure 6. Antiangiogenic effect exerted by RERF in mice. A and B, Matrigel-containing angioreactors loaded with diluents (PBS), 10 nmol/L SRSRY, 12.5 ng VEGF mixed to PBS, 10 nmol/L RERF, or 10 μg/mL endostatin (End) were implanted subcutaneously into the dorsal flank of 12 CD1 nude mice (2 angioreactors/mouse). Fifteen days after the implantation, mice were sacrificed and angioreactors were removed. Representative macroscopic view of the resulting angioreactors. B, quantification of the endothelial cells in the developed vasculature 15 days after implantation. The extracellular matrix was removed from each cylinder and the endothelial cells, recovered by dispase digestion and labeled with FITC-lectin, were quantified by fluorescence at 510 nm emission with 485 nm excitation using a fluorimeter. Box plots represent data from a total of 2 experiments each with 4 angioreactors/sample. The median values are indicated. C, corneal pocket assay in 12 female New Zealand White rabbits. Sucralfate hydron pellets impregnated with diluents (PBS), 5 μg RERF, 180 ng VEGF, or a mixture of 180 ng VEGF and 5 μg RERF were implanted in rabbit corneas. Representative stereomicroscopy images recorded 15 day after pellet implantation. D, quantification of the angiogenic score (1 corresponded to 0–25 vessels per cornea, 2 from 25–50, 3 from 50–75, 4 from 75–100, and 5 for >100 vessels). Plots represent data from a total of 6 eyes per sample. The median values are indicated. E, HT1080 cells were injected subcutaneously in the flanks of 10 nude mice. The day after, the mice were randomized into 2 groups (5 animals/group), and treatments were started. Control mice received PBS alone, whereas experimental group received i.v. injection of 3 μg/kg RERF every other day. Comparative images of a mouse treated with vehicle or RERF recorded after 10 and 20 days are depicted. F, tumor volume was measured at various time points with a caliper, using the formula: $^1/_2 \times (\text{width})^2 \times \text{length}$. G, after 20 days, animals were sacrificed and excised tumors were fixed in buffered formalin and processed for paraffin sectioning. Representative images from sections stained with hematoxylin and eosin to visualize vascular channels harboring red blood cells (arrows). H, tumor vascularization was assessed by counting vessels on hematoxylin and eosin–stained sections in 5 randomly chosen fields per section, in at least 2 sections per tumor at ×200 magnification.

of endothelial cell-associated fluorescence revealed that angioreactors loaded with VEGF/RERF or SRSRY/RERF retained 15% and 8% of fluorescence recovered by angioreactors loaded with VEGF or SRSRY, respectively (Fig. 6B). Noticeably, antiangiogenic effects exerted by RERF and endostatin in the presence of VEGF were comparable (angiogenesis reduced to 15% and 11%, respectively; Fig. 6B). Furthermore, antiangiogenic activity of RERF was investigated by a corneal pocket assay in rabbits. Neovascular growth was evaluated in 12 rabbits upon subcorneal implantation of slow release pellets containing PBS or 180 ng VEGF with/without 5 μg RERF. Implantation of pellets containing 180 ng VEGF stimulated ingrowth of blood vessels in the rabbit corneas starting from day 2 and continuing to grow progressively up to 15 days before regressing. At day 15, rabbit corneas probed with pellets impregnated with VEGF exhibited higher angiogenic score then the average score of those impregnated with vehicle (PBS; 3.3 ± 0.5 vs. 0.1 ± 0.2 with $P < 0.0001$). RERF was tested at 5 μg/pellet alone, to evaluate its potential inflammatory response and in the presence of VEGF (180 ng/pellet). RERF produced a 69.7% inhibition of VEGF-induced vascularization (1 ± 0,6 vs. 3.3 ± 0.5 with $P < 0.001$), without eliciting inflammation (Fig. 6C and D). Taken together, our findings indicate that RERF behaves as an antiangiogenic factor which prevents not only $uPAR_{88–92}$–induced but also VEGF-induced angiogenesis *in vivo*. Finally, we investigated whether RERF exerts such effect on tumor growth using xenograft models using highly invasive and VEGF-producing HT1080

cells (39). Treatments with vehicle (PBS) or RERF (3 mg/kg) started the day after the implantation and continued every other day. Mice weight was monitored, and time-dependent average weight increase showed that the animals survived the treatment schedule without changes in body weight. After 20 days, all mice were sacrificed, tumors were excised, and vascular channels harboring red blood cells were counted on hematoxylin and eosin–stained sections. The HT1080 cells readily formed tumors when injected subcutaneously in the flanks of the immunocompromised mice (Fig. 6E). The measurement of tumor volume at various time points showed that the kinetics of tumor formation in vehicle-treated mice were significantly higher than those assessed in RERF-treated mice. After 20 days, tumor volumes of vehicle-treated mice were 862 ± 104 and 476 ± 121 mm^3, respectively, with $P < 0.001$ (Fig. 6F). Furthermore, microvessel density was reduced in tumors from animals treated with RERF as compared with those treated with vehicle alone (Fig. 6G and H). Overall, these findings confirmed that RERF is a promising therapeutic agent for the control of diseases sustained by excessive angiogenesis such as cancer.

Discussion

This work is based on previous evidence showing that the uPAR chemotactic sequence ($uPAR_{88–92}$) drives *in vitro* and *in vivo* angiogenesis in a protease-independent manner (20). On this basis, we investigated whether endothelial cells are sensitive to synthetic peptides which were previously shown to inhibit the $uPAR_{88–92}$–dependent signals (24, 25). Now we show that RERF also inhibits angiogenesis driven by VEGF, a widely recognized central factor in new vessel formation. Here, we report that RERF prevents *in vitro* migration and tube formation by endothelial cells exposed to VEGF and counteracts VEGF-induced phosphorylation of many proteins such as FAK. Furthermore, RERF has been proven to prevent cytoskeletal reorganization, cell adhesion onto vitronectin, and the recruitment of αvβ3 integrin at the focal adhesions of endothelial cells exposed to VEGF. Antiangiogenic effects exerted by RERF are reproducible *in vivo* when Matrigel-containing angioreactors were implanted in nude mice as well as when neovascularization was induced by subcorneal implantation in rabbits of slow release pellets containing VEGF. Finally, analyses of growth and vascularization of tumors formed by HT1080 cells implanted in nude mice clearly support the inhibitory activity of RERF on angiogenesis. While the effects of RERF on $uPAR_{88–92}$–driven angiogenesis were to be expected, the effects of RERF on VEGF-induced angiogenesis were not. Our findings unravel a more complex picture of the effects of RERF on endothelial cells and, more generally, highlight the role of uPAR, FPR, integrins, and VEGF-induced signaling events in the regulation of endothelial cell functions.

uPAR is documented to be a key component of the network through which VEGF controls endothelial cell migration (10). Here, we present evidence that RERF inhibits VEGF-triggered migration and cord-like formation of endothelial cells in a dose-dependent manner, maximal effect being reached at 10 nmol/L. Although we have not yet identified the exact molecular mechanism, our findings indicate that RERF prevents VEGF-dependent phosphorylation of downstream mediators such as Src, PlCγ-1, Akt, extracellular signal–regulated kinase (ERK)1/2, and FAK, all required for VEGF-mediated angiogenesis (37). Intriguingly, most of these are recognized mediators also of uPAR-triggered signaling (40). Thus, it is difficult to pinpoint the exact sequence of events and the contribution of each subset of mediators in the inhibitory effects exerted by RERF.

Our previous work has documented that RERF prevents in endothelial cells uPAR/FPR and uPAR/αv interactions, mainly by binding to the G-protein–coupled receptor FPR (K_{dapp}, 10^{-17} mol/L) and αv (K_{dapp}, 10^{-13} mol/L), respectively (20, 25). In the experiments presented here, the RERF-dependent inhibitory effects on endothelial cell migration and tube formation start in the femtomolar range, suggesting that both proximal interactions may be occurring. Interestingly, inhibitory effect of RERF on VEGF-directed cell migration was dramatically reduced when endothelial cells were desensitized with 100 nmol/L fMLP, indicating that FPR activity is required for RERF function. Furthermore, the involvement of αvβ3 integrin is supported by the findings that cell adhesion to vitronectin and the extent of αvβ3 complexed with VEGFR2 are greatly reduced in the presence of RERF. On the other hand, the pivotal role of αvβ3 in mediating $uPAR_{88–92}$ signaling as well as VEGF-dependent proangiogenic stimulus is well-established (12, 13, 36). In particular, the $uPAR_{88–92}$–dependent proangiogenic effect occurs through the assembly of uPAR in composite regulatory units with αvβ3 integrin and FPR (20).

Taken together, our results confirm the involvement of FPR in binding and mediating inhibition by RERF and suggest a mechanism by which αvβ3 is either directly (via integrin interaction) or indirectly (via FPR interaction) forced into an inactive state by RERF and, consequently, VEGFR2 as well as downstream signaling mediators are not activatable. In this view, the αvβ3 vitronectin receptor represents a common mediator between the uPAR, acting through its $uPAR_{88–92}$ chemotactic epitope and VEGFR2 systems.

The neovascularization of malignant tumors is a critical step in their growth and spread, and the pharmacologic control of this process is considered one of the most promising approaches for the treatment of neoplastic diseases. However, the results are more modest than predicted by most preclinical testing and benefits in progression-free survival are frequently not accompanied by overall survival improvements (5). Furthermore, several side effects have been ascribed to antiangiogenic drugs such as bevacizumab that significantly increases the risk of cardiac ischemic events in patients with cancer (41). Therefore, improved drugs are needed. With respect to this, RERF is a good drug by virtue of its ability to selectively inhibit integrin/VEGFR2 cross talk and FPR

unlike bevacizumab, indicating that RERF behaves differently from other VEGF inhibitors. This suggests a potentially wider but still target-specific activity for RERF.

In tumors, an excess of VEGF induces "vessel abnormalization," characterized by a disorganized, chaotic microvascular network of tortuous immature vessels. Endothelium becomes "abnormalized," leading to an increase of interstitial fluid pressure with consequent vessel collapse (42). An interesting point will be to analyze how RERF is able to revert such effects.

Evidence indicating the role of the uPA/uPAR system in the regulation of the innate immune system in the inflammation process, of the adaptive immune response, as well as the role of fibrin and fibrin degradation products at the cross-road between coagulation and inflammation does exist (43). Furthermore, FPRs are documented to regulate innate inflammatory responses and mediate cell migration in response to a variety of chemotactic factors by facilitating the trafficking of phagocytes to the site of bacterial invasion (44). Given the finding that RERF interferes with the complex cross-talk involving uPAR, FPR, and integrins, it is reasonable to foresee that this peptide may be also used to develop new drugs for the treatment of diseases that are sustained by a chronic excess of cell migration such as inflammatory diseases. The uPA/uPAR system is not only regarded as one of the key systems driving tumor invasion and metastases but is also now appearing as an essential component of the network through which VEGF controls angiogenesis. To date, different strategies to prevent the interaction of uPAR with integrins have been designed (45). In the new frame, RERF could be considered a unique and valid prototype for the development of new antineoplastic therapies designed to simultaneously counteract tumor cell dissemination and intra-tumoral neovascularization.

Disclosure of Potential Conflicts of Interest

No potential conflicts of interest were disclosed.

Authors' Contributions

Conception and design: K. Bifulco, M. De Rosa, V. Pavone, M.V. Carriero
Development of methodology: K. Bifulco, I. Longanesi-Cattani, E. Liguori, C. Arra, D. Rea
Acquisition of data (provided animals, acquired and managed patients, provided facilities, etc.): C. Arra, D. Rea
Analysis and interpretation of data (e.g., statistical analysis, biostatistics, computational analysis): K. Bifulco, I. Longanesi-Cattani, M.T. Masucci, M.P. Stoppelli
Writing, review, and/or revision of the manuscript: M. De Rosa, V. Pavone, M.P. Stoppelli, M.V. Carriero
Administrative, technical, or material support (i.e., reporting or organizing data, constructing databases): E. Liguori, M.T. Masucci
Study supervision: M.V. Carriero

Acknowledgments

The authors thank Dr Marie Ranson for critical review of the manuscript and Gioconda Di Carluccio is for her technical assistance.

Grant Support

This work was supported by AIRC (Associazione Italiana per la Ricerca sul Cancro) 2010, project 10251 (M.V. Carriero) and by Italian Ministry of Health RF-2010-2316780 (M.V. Carriero).

The costs of publication of this article were defrayed in part by the payment of page charges. This article must therefore be hereby marked *advertisement* in accordance with 18 U.S.C. Section 1734 solely to indicate this fact.

Received February 4, 2013; revised July 18, 2013; accepted August 3, 2013; published OnlineFirst August 12, 2013.

References

1. Carmeliet P, Jain RK. Angiogenesis in cancer and other diseases. Nature 2000;407:249–57.
2. Aguirre-Ghiso JA. Models, mechanisms and clinical evidence for cancer dormancy. Nat Rev Cancer 2007;7:834–46.
3. Folkman J. Tumor angiogenesis: therapeutic implications. N Engl J Med 1971;285:1182–6.
4. Ferrara N, Kerbel RS. Angiogenesis as a therapeutic target. Nature 2005;438:967–74.
5. Ebon JM, Kerbel RS. Antiangiogenic therapy: impact on invasion, disease progression, and metastasis. Nat Rev Clin Oncol 2011;8:210–21.
6. Cébe-Suarez S, Zehnder-Fjällman A, Ballmer-Hofer K. The role of VEGF receptors in angiogenesis; complex partnerships. Cell Mol Life Sci 2006;63:601–15.
7. Lamalice L, Le Boeuf F, Huot J. Endothelial cell migration during angiogenesis. Circ Res 2007;100:782–94.
8. Eliceiri BP, Cheresh DA. Adhesion events in angiogenesis. Curr Opin Cell Biol 2001;13:563–8.
9. Brooks PC, Clark RA, Cheresh DA: Requirement of vascular integrin alpha v beta 3 for angiogenesis. Science 1994;264:569–71.
10. Alexander RA, Prager GW, Mihaly-Bison J, Uhrin P, Sunzenauer S, Binder BR, et al. VEGF-induced endothelial cell migration requires urokinase receptor (uPAR)-dependent integrin redistribution. Cardiovasc Res 2012;94:125–35.
11. Ploug M, Rønne E, Behrendt N, Jensen AL, Blasi F, Danø K. Cellular receptor for urokinase plasminogen activator. Carboxyl-terminal processing and membrane anchoring by glycosyl-phosphatidylinositol. J Biol Chem 1991;266:1926–33.
12. Smith HW, Marshall CJ. Regulation of cell signaling by uPAR. Nat Rev Mol Cell Biol 2010;11:23–36.
13. Blasi F, Carmeliet P. uPAR: a versatile signaling orchestrator. Nat Rev Mol Cell Biol 2002;3:932–43.
14. Sidenius N, Blasi F. The urokinase plasminogen activator system in cancer: recent advances and implication for prognosis and therapy. Cancer Metastasis Rev 2003;22:205–22.
15. Shariat SF, Roehrborn CG, McConnell JD, Park S, Alam N, Wheeler TM, et al. Association of the circulating levels of the urokinase system of plasminogen activation with the presence of prostate cancer and invasion, progression, and metastasis. J Clin Oncol 2007;25:349–55.
16. Henic E, Borgfeldt C, Christensen IJ, Casslén B, Høyer-Hansen G. Cleaved forms of the urokinase plasminogen activator receptor in plasma have diagnostic potential and predict postoperative survival in patients with ovarian cancer. Clin Cancer Res 2008;14:5785–93.
17. Rasch MG, Lund IK, Almasi CE, Hoyer-Hansen G. Intact and cleaved uPAR forms: diagnostic and prognostic value in cancer. Front Biosci 2008;13:6752–62.
18. Binder BR, Mihaly J, Prager GW. uPAR-uPA-PAI-1 interactions and signaling: a vascular biologist's view. Thromb Haemost 2007;97:336–42.
19. Pepper MS. Role of the matrix metalloproteinase and plasminogen activator-plasmin systems in angiogenesis. Arterioscler Thromb Vasc Biol 2001;21:1104–17.
20. Bifulco K, Longanesi-Cattani I, Gala M, DI Carluccio G, Masucci MT, Pavone V, et al. The soluble form of urokinase receptor promotes angiogenesis through its Ser^{88}-Arg-Ser-Arg-Tyr^{92} chemotactic sequence. J Thromb Haemost 2010;8:2789–99.

21. Resnati M, Pallavicini I, Wang JM, Oppenheim J, Serhan CN, Romano M, et al. The fibrinolytic receptor for urokinase activates the G protein-coupled chemotactic receptor FPRL1/LXA4R. Proc Natl Acad Sci USA 2002;99:1359–64.
22. Gargiulo L, Longanesi-Cattani I, Bifulco K, Franco P, Raiola R, Campiglia P, et al. Cross-talk between fMLP and vitronectin receptors triggered by urokinase receptor-derived SRSRY peptide. J Biol Chem 2005;280:25225–32.
23. Bifulco K, Longanesi-Cattani I, Franco P, Pavone V, Mugione P, Di Carluccio G, et al. Single amino acid substitutions in the chemotactic sequence of urokinase receptor modulate cell migration and invasion. PLoS One 2012;7:e44806.
24. Bifulco K, Longanesi-Cattani I, Gargiulo L, Maglio O, Cataldi M, De Rosa M, et al. An urokinase receptor antagonist that inhibits cell migration by blocking the formyl peptide receptor. FEBS Lett 2008;582:1141–6.
25. Carriero MV, Longanesi-Cattani I, Bifulco K, Maglio O, Lista L, Barbieri A, et al. Structure-based design of an urokinase-type plasminogen activator receptor-derived peptide inhibiting cell migration and lung metastasis. Mol Cancer Ther 2009;8:2708–17.
26. Arnaoutova I, Kleinman HK. In vitro angiogenesis: endothelial cell tube formation on gelled basement membrane extract. Nat Protoc 2010; 5:628–35.
27. Masucci MT, Pedersen N, Blasi F. A soluble, ligand binding mutant of the human urokinase plasminogen activator receptor. J Biol Chem 1991;266:8655–8.
28. Carriero MV, Franco P, Del Vecchio S, Massa O, Botti G, D'Aiuto G, et al. Tissue distribution of soluble and receptor-bound urokinase in human breast cancer using a panel of monoclonal antibodies. Cancer Res 1994;54:5445–54.
29. O'Reilly MS, Boehm T, Shing Y, Fukai N, Vasios G, Lane WS, et al. Endostatin: an endogenous inhibitor of angiogenesis and tumor growth. Cell 1997;88:277–85.
30. Yang S, Graham J, Kahn JW, Schwartz EA, Gerritsen ME. Functional roles for PECAM-1 (CD31) and VE-cadherin (CD144) in tube assembly and lumen formation in three-dimensional collagen gels. Am J Pathol 1999;155:887–95.
31. Limame R, Wouters A, Pauwels B, Fransen E, Peeters M, Lardon F, et al. Comparative analysis of dynamic cell viability, migration and invasion assessments by novel real-time technology and classic endpoint assays. PLoS One 2012;7:e46536.
32. Guedez L, Rivera AM, Salloum R, Miller ML, Diegmueller JJ, Bungay PM, et al. Quantitative assessment of angiogenic responses by the directed *in vivo* angiogenesis assay. Am J Pathol 2003;162: 1431–9.
33. Mohan RR, Tovey JCK, Sharma A, Schultz GS, Cowden JW, Tandon A. Targeted decorin gene therapy delivered with adeno-associated virus effectively retards corneal neovascularization *in vivo*. PLoS One 2011;6:e26432.
34. Rousseau S, Houle F, Huot J. Integrating the VEGF signals leading to actin-based motility in vascular endothelial cells. Trends Cardiovasc Med 2000;10:321–7.
35. Kowanetz M, Ferrara N. Vascular endothelial growth factor signaling pathways: therapeutic perspective. Clin Cancer Res 2006;12: 5018–22.
36. Mahabeleshwar GH, Feng W, Reddy K, Plow EF, Byzova TV. Mechanisms of integrin-vascular endothelial growth factor receptor cross-activation in angiogenesis. Circ Res 2007;10:570–80.
37. Soldi R, Mitola S, Strasly M, Defilippi P, Tarone G, Bussolino F. Role of $\alpha v\beta 3$ integrin in the activation of vascular endothelial growth factor receptor-2. EMBO J 1999;18:882–92.
38. Zachary I, Gliki G. Signaling transduction mechanisms mediating biological actions of the vascular endothelial growth factor family. Cardiovasc Res 2001;49:568–81.
39. Misra RM, Bajaj MS, Kale VP. Vasculogenic mimicry of HT1080 tumor cells *in vivo*: critical role of HIF-1α-neuropilin-1 axis. PLoS One 2012;7: e50153.
40. D'Alessio S, Blasi F. The urokinase receptor as an entertainer of signal transduction. Front Biosci 2009;14:4575–87.
41. Ranpura V, Hapani S, Chuang J, Wu S. Risk of cardiac ischemia and arterial thromboembolic events with the angiogenesis inhibitor bevacizumab in cancer patients: a meta-analysis of randomized controlled trials. Acta Oncol 2010;49:287–97.
42. Carmeliet P, De Smet F, Loges S, Mazzone M. Branching morphogenesis and antiangiogenesis candidates: tip cells lead the way. Nat Rev Clin Oncol 2009;6:315–26.
43. Del Rosso M, Margheri F, Serratì S, Chillà A, Laurenzana A, Fibbi G. The urokinase receptor system, a key regulator at the intersection between inflammation, immunity, and coagulation. Curr Pharm Des 2011;17: 1924–43.
44. Gavins FNE. Are formyl peptide receptors novel targets for therapeutic intervention in ischaemia-reperfusion injury? Trends Pharmacol Sci 2010;31 266–76.
45. Carriero MV, Stoppelli MP. The urokinase-type plasminogen activator and the generation of inhibitors of urokinase activity and signalling. Curr Pharm Des 2011;17:1944–61.